Journal of Drug Delivery Science and Technology 91 (2024) 105097

Contents lists available at ScienceDirect

Journal of Drug Delivery Science and Technology

journal homepage: www.elsevier.com/locate/jddst

Solid lipid nanoparticles for efficient delivery of capsaicin-rich extract: Potential neuroprotective effects in Parkinson's disease

Lisa Marinelli [a], Marilisa Pia Dimmito [a,*], Ivana Cacciatore [a], Eleonora Chiara Toto [a], Annalisa Di Rienzo [a], Ferdinando Palmerio [a], Valentina Puca [a], Ester Sara Di Filippo [b], Stefania Fulle [b], Antonio Di Stefano [a]

[a] University "G. D'Annunzio" of Chieti-Pescara, Department of Pharmacy, Via Dei Vestini 31, 66100, Chieti, Italy
[b] University "G. D'Annunzio" of Chieti-Pescara, Department of Neuroscience Imaging and Clinical Sciences, 66100, Chieti, Italy

ARTICLE INFO

Keywords:
Capsaicin
Controlled release
Drug delivery
Parkinson's disease
Solid lipid nanoparticle

ABSTRACT

Parkinson's disease (PD) is a debilitant neurodegenerative disease that unveils severe physical, and psychological burdens on patients. To date, there is no effective treatment capable of inverting the disease course, freezing the cognitive impairment, and other non-motor features. Solid lipid nanoparticles (SLNs) can represent a promising approach to provide safe and site-specific delivery of naturally occurring compounds counteracting PD symptoms. In this work, SLNs were purposed for the release of a capsaicin-rich extract (CPS-extract) and investigated for their efficacy in PD pathology. SLNs were prepared by using stearic acid (SA) and Brij 78 as lipid and surfactant, respectively. Different formulation parameters, including drug: lipid ratio and surfactant concentrations were investigated. The selected formulation brings together particle sizes of around 200 nm, high encapsulation efficiency (>80 %), and provides 90 % of CPS release within 24 h, which well fits in the Kosermayer-Peppas model. Differential Scanning Calorimetry (DSC) analysis confirmed the presence of the lipid in the solid crystalline state, while stability studies revealed that CPS-extract SLNs preserve their stability for at least 30 days. Moreover, biological assays, performed on retinoic acid/phorbol 12-myristate 13-acetate (RA/PMA) differentiated SH-SY5Y neuroblastoma cell line, revealed that CPS-extract SLNs possessed a significant protective effect in reducing reactive oxygen species (ROS) increments induced by the neurotoxic agent H_2O_2.

1. Introduction

Parkinson's disease (PD) is a fast-growing neurodegenerative disorder, widespread primarily in the geriatric population, associated with motor dysfunctions (rigidity, tremor, and gradualness of movement) depending on the progressive degeneration of nigrostriatal dopamine (DA) neurons. Despite the major advances in this field, the aetiology of PD remains an unsolved issue and a PD model useful to estimate the effect of drugs on the disease progression is lacking [1]. Most of the existing PD treatments are based on the restoration of dopaminergic tone in the striatal nucleus but they often result inadequate [2]. Existing therapeutics are ineffective and intended to mitigate cognitive and behavioural symptoms. In fact, to date, there is no successful treatment capable of inverting the disease course, freezing the cognitive impairment, and other symptoms, affecting the patient's quality of life [3]. One of the major limiting factors of available PD pharmacological treatments is the poor brain bioavailability due to the blood-brain barrier (BBB) which restricts central nervous system (CNS) targeting. Moreover, neuropsychiatric side effects represent a further criticism of conventional synthetic drugs [4]. Recently, plant-derived natural products and plant extracts have been investigated for their therapeutic potential. They claim simple accessibility, affordability, safety, and neurodegenerative-protecting properties [5]. Among them, Capsaicin (CPS), chemically composed of an aromatic ring and a hydrophobic chain connected through a polar amide group [6], is an alkaloid belonging to the vanilloids family, extracted from chili pepper (Fig. 1). CPS possesses anti-cancer, analgesic, antioxidant, antimicrobial, antifungal, cardioprotective, and anti-obesity activities [7,8]. Moreover, its beneficial effect in the prevention and management of neurodegenerative diseases is also proved. In a 1-methyl-4-phenyl-1,2,3,6-tetrahydropyridine (MPTP) mouse model of PD, CPS displayed capability in inhibiting brain inflammation and oxidative stress by activation of the

* Corresponding author.
E-mail address: marilisa.dimmito@unich.it (M.P. Dimmito).

https://doi.org/10.1016/j.jddst.2023.105097
Received 14 June 2023; Received in revised form 11 October 2023; Accepted 24 October 2023
Available online 30 October 2023
1773-2247/

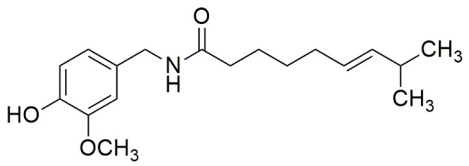

Fig. 1. Chemical structure of Capsaicin.

transient receptor potential vanilloid subtype 1 (TRPV1), highly expressed in the brain, which modulates neuronal function and controls motor behavior. Indeed, TRPV1 receptors stimulation led to a sequence of events that involve astrocyte activation and result in increased DA levels in the striatum [9]. Literature data show that CPS when intraperitoneally administered in PD mouse model can increase the number of dopaminergic neurons in the substantia nigra, also shifting the microglial cells to an anti-inflammatory state [10–12]. Furthermore, dietary CPS increases dopamine content in the transgenic *Drosophila* expressing human α-synuclein, reducing the markers of oxidative stress, and enhancing free radical scavenging [13]. Notwithstanding literature data highligh the effectiveness of CPS, its applicability is hampered by poor water solubility, pungency-induced irritation, off-target effects, a high degree of first-pass metabolism, and low bioavailability of about 2–20 % [14,15]. Several studies have been reported regarding the development of novel formulations that ameliorate CPS-associated drawbacks, including liposomes, hydrogels, and nanoformulations. For example, CPS-loaded alginate nanoparticles loaded in polycaprolactone-chitosan nanofibers exhibit an improved prolonged release of CPS from 120 h to 500 h [15]. While CPS-loaded folic acid-conjugated lipid nanoparticles prevented rapid RES uptake prolonging their blood circulation time [16]. Kunjiappan and coworkers reported CPS-loaded solid lipid nanoparticles with anticancer efficacy on human hepatocellular carcinoma *in vitro* [17]. Notably, nanotechnology has been explored as a useful strategy to modify poor physico-chemical properties and facilitate transport across the BBB [18–20]. Among various colloidal systems, solid lipid nanoparticles (SLNs) have received special interest due to many features that make them particularly captivating as alternative drug carriers, being able to trap and safeguard drugs in the biocompatible core [21,22]. SLNs may represent a valid delivery platform since possessing countless advantages mostly due to the reduced nanosized dimensions that allow bypassing the liver and spleen filtration prolonging blood circulation and allowing them to reach the site of interest [23]. Drug-loaded SLNs highlight sustained release features, and, due to biodegradable constituents, lower toxicity than polymeric nanoparticles [22]. Since evidence of herbal-extract nanoformulations reaching the central nervous system (CNS) exists but only a few examples of nanoformulations loaded with CPS-extract are described, in the present work, we reported the preparation of SLNs loaded with a CPS-extract obtained from *Capsicum annuum* fruits and we evaluated their potential applicability in the treatment of CNS disorders. To improve the drug-likeness profile of CPS, CPS-extract SLNs were purposed for a potential oral administration. They were prepared, characterized for their physicochemical properties as well as entrapment efficiency, drug release, and evaluated for the *in vitro* biological activity assessed by dichloro-dihydro-fluorescein diacetate (DCFH-DA) assay on retinoic acid/phorbol 12-myristate 13-acetate (RA/PMA) differentiated SH-SY5Y neuroblastoma cell line. According to our findings, there is no literature data, on drug delivery systems based on SLNs loaded with CPS-extract for application in the field of neurodegenerative disorders.

2. Experimental section

2.1. Materials

Stearic acid (SA), polyoxyethylen (20) stearyl ether (Brij 78), ethanol, capsaicin standard, tween 80, dodecane, dopamine, diazepam, Dulbecco's Modified Eagle's medium, heat-inactivated fetal bovine serum, penicillin, streptomycin, L-glutamine, retinoic acid, phorbol 12-myristate 13-acetate. 3-[4,5-dimethylthiazol-2-yl]-2,5-diphenyltetrazolium bromide, hydrogen peroxide, nitro blue tetrazolium chloride, 2′,7′-dichlorofluorescin diacetate (H_2DCF-DA), dimethyl sulfoxide (DMSO), Milli-Q water, methanol, acetonitrile, MultiScreen-IP PAMPA filter plate and 96-well polytetrafluoroethylene (PTFE) plate were purchased from Sigma-Aldrich (St. Louis, MO, USA). Porcine polar brain lipid (PBL) extract was acquired from Avanti Polar Lipids, Inc. CPS was extracted from *Capsicum annuum* fruits.

2.2. Capsicum annuum extraction

CPS was extracted from *Capsicum annuum* L. fruits collected in Pescara, Italy (42.4618° N, 14.2161° E). After the peduncle and seeds separation, fruits were dried under atmosphere conditions until reaching a constant weight and then powdered using an electric blender. The finely triturated powder (400 Mesh) was stored at −20 °C before being subjected to the extraction procedure, accomplished by hot maceration in ethanol, under vigorous stirring for 3h at 50 ± 0.5 °C. The dark red extraction mixture was filtered, dried, and characterized by High-Performance Liquid Chromatography (HPLC) analysis.

2.3. Chromatographic conditions

The chromatographic analyses were performed using an Agilent 1260 Infinity II HPLC (Agilent, Santa Clara, CA, USA) consisting of a 1260 Infinity II Quaternary Pump (model G7111A), 1260 Infinity II auto-sampler (model G7129A), a 1260 Infinity II Multicolumn Thermostat (model G7116A), and a 1260 Infinity II Diode Array Detector (model G7115A) equipped with a Poroshell 120 EC-C18 column (150 × 4.6 mm i.d., particle size 4 μm, Agilent, Santa Clara, USA) operating at 20 °C. The samples were analyzed in isocratic elution mode using a mixture of acetonitrile (A) and water (B) 50:50 *v/v*, for 30 min, at a flow rate of 0.8 mL/min, with a UV detector set at 280 nm. Starting from a CPS stock solution in methanol (10 mg/mL), a series of dilutions, in the range of 2.5–50 μg/mL, were used for the calibration curve. The LOD and LOQ were determined based on the equations: LOD = 3.3 × σ/S and LOQ = 10 × σ/S, where σ is the standard deviation of the intercept with y-axis and S the slope [24].

2.4. Preparation of CPS-extract SLNs

Preformulation studies for CPS-extract SLNs were performed using different CPS-extract/lipid ratios (1:2, 1.5:1, 2:1 *w/w*). To select the best formulation, physico-chemical features such as the mean particle size, polydispersity index (PDI), and ζ-potential were considered. SLNs were prepared according to a procedure that involved first an emulsification phase followed by the evaporation and the subsequent solidifying step [18]. Briefly, SA (33.6 mg) was dissolved in 2.5 mL of pure ethanol under stirring at 40 ± 2 °C. Simultaneously, an aqueous phase (24 mL), containing Brij 78 (12.68 mg) as surfactant, was heated at 70 ± 2 °C. Under mechanical stirring (400 rpm), the organic phase was added drop by drop to the aqueous phase. The so-obtained lipid emulsion was left at 70 ± 2 °C under stirring for the complete organic solvent removal and then diluted with an equal volume of cold water to allow the nanoparticle solidification. In CPS-extract SLNs, the SA and the CPS-extract, containing 2 % *w/w* of CPS (44 mg), were both dissolved in the organic phase. To remove the unentrapped drug, the final suspension was filtered through a 1.20 μm syringe filter (Minisart Plus).

2.5. Physico-chemical properties of CPS-extract SLNs

Formulations were characterized in terms of particle size and PDI by dynamic light scattering (DLS, Anton Paar Litesizer 500 Graz, Austria).

Samples were diluted 1:10 with Milli-Q water in a 1.5-mL disposable cuvette. Samples were thermostated for 2 min at 25 °C before each measurement which was performed at 25 °C in back scattering mode (175°). Results reported as mean hydrodynamic diameter were obtained from three repetitions per sample in triplicate. The ζ-potential was measured by the electrophoretic light scattering (AntonPaar Litesizer 500, Graz, Austria). The samples were conditioned in an electrophoretic Omega cuvette Mat. No. 225288 at 25 °C, applying a potential of 200.0 V. The ζ-potential values of CPS-extract, empty and extract-loaded SLNs were calculated from the electrophoretic mobility obtained from 12 repeated analyses via the conversion of electrophoretic mobility according to the method used by Helmholtz-von Smoluchowski.

2.6. Encapsulation efficiency (EE%)

The EE% was determined by a direct method. 100 μL of CPS-extract SLNs as colloidal dispersion was added to 900 μL of methanol, vortexed, and sonicated to allow the nanoparticle disruption. The obtained solution was filtered through a 0.45 μm syringe filter and analyzed by HPLC, to quantify the entrapped CPS [25]. The EE% was obtained by the ratio of the found and theoretical amount of CPS encapsulated in SLNs. The yield of the preparation process of SLNs was calculated as the weight of the product obtained after the freeze-drying compared to the weight of the different components used during the formulation set-up. The encapsulation efficiency percentage (EE %) was calculated by using equation (1):

$$EE\ \% = \left(\frac{Wf}{Wt}\right) * 100 \quad (1)$$

where *Wf* is the amount of CPS found and *Wt* is the total amount of loaded CPS [26].

2.7. Differential scanning calorimetry (DSC)

DSC analysis was performed using an instrument PerkinElmer Inc. (Waltham, MA, USA) in the temperature ranging from 20 to 200 °C in hermetically sealed aluminum capsules. Briefly, the pan was filled with 5 mg of each sample, and heated with a scan rate of 10 °C/min. An empty pan with a cover was used as a reference. The DSC measurements were carried out for the following samples: (a) SA; (b) CPS-extract; (c) Brij 78; (d) empty SLNs; and (e) CPS-extract SLNs.

2.8. Storage stability of CPS-extract SLNs

Formulation stability was determined after incubation at 25 ± 2 °C and 4 ± 2 °C over a period of 30 days. The formulations were stored in a colourless glass, sealed vial. At each time point (0, 3, 4, 5, 6, 10, 20, 30 days) the formulations were assessed in terms of physico-chemical parameters such as size, ζ-potential, PDI, and EE%.

2.9. In vitro release profile

CPS release was determined using a dialysis bag (Pur-A-Lyzer Mega 12000 kDa MWCO, Sigma-Aldrich, St. Louis, MO, USA) which guarantees the CPS-extract diffusion, avoiding the SLNs passage. 15 mL of the CPS-extract SLNs were introduced in the dialysis bag and maintained at 37 ± 0.5 °C, under continuous stirring at 500 rpm to ensure homogeneity of the system. Experiments were performed under sink conditions using 600 mL of release medium composed of 200 mM phosphate buffer solution (PBS, pH 7.4) enriched with 0.05 % of tween 80. At predefined time intervals, aliquots (100 μL) of the incubated CPS-extract SLNs were sampled from the dialysis bag, diluted 1:10 with methanol, and following the same procedure used for the EE% determination, CPS, was quantified by HPLC. The cumulative release was calculated by determining the residual CPS quantity in the donor compartment ($n = 3$), following equation (2):

$$Cumulative\ percentage\ release\ \% = \left(\frac{Volume\ of\ sample\ withdrawn\ (mL)}{Bath\ volume}\right) * P(t-1) + Pt \quad (2)$$

where Pt = percentage released at time t and P (t-1) is the percentage released before t [27].

The zero-, first order, Higuchi, and Korsmeyer-Peppas models were applied to ascertain the CPS release kinetic from the SLNs. The best-fitting one was defined considering the highest regression values (R^2) of the analyzed release data. Moreover, the *n* value, obtained from the slope of the equation referring to the Korsmeyer-Peppas model, was employed to define the release mechanism of CPS as well [28].

2.10. Parallel artificial membrane permeation assay (PAMPA)

The PAMPA method was used to evaluate the CPS BBB permeability. Analyses were performed using a 96-well, MultiScreen-IP PAMPA filter plate as donor, and a 96-well polytetrafluoroethylene (PTFE) acceptor plate as receiving. Donor wells were treated with a lipid solution prepared in *n*-dodecane (2 % *w/v*) based on porcine polar brain lipid (PBL) extract (from Avanti Polar Lipids, Inc.). Donor solution consisting of CPS, CPS-extract, and CPS-extract SLNs were diluted with PBS (pH 7.4) supplemented with DMSO (5 % *v/v*) to reach a final CPS concentration of 100 μg/mL. The acceptor solution had the same composition as the donor but without the investigated compounds. The system was assembled by setting 300 μL of the donor and acceptor solutions between an artificial membrane, previously coated, with a solution (5 μL) of the phospholipid mixture. After 18 h of incubation, concentrations in each donor and acceptor well were quantified by HPLC, and the effective permeability coefficient (*Pe*, cm/s) was calculated as previously reported [29]. To assess the suitability and reliability of the system, dopamine, and diazepam were used as reference compounds with low and high BBB permeability, respectively [30].

2.11. Biological studies

2.11.1. SH-SY5Y cell culture

Human SH-SY5Y neuroblastoma cells (EGACC, Sigma–Aldrich, UK) were grown in Dulbecco's Modified Eagle's medium supplemented with 10 % heat-inactivated fetal bovine serum, penicillin (100 U/mL), streptomycin (100 μg/mL), and 1 % L-glutamine. The cells were maintained at 37 °C in a 5 % CO_2 humidified atmosphere. To obtain a dopaminergic phenotype, the SH-SY5Y cells were treated with retinoic acid (RA)/phorbol 12-myristate 13-acetate (PMA). In detail, the medium was supplemented with RA (10 μM) for 3 days; then the medium was removed and replaced with a growth medium containing PMA (80 nM) for a subsequent 3 days.

2.11.2. MTT assay

2700 cells/well were seeded in a final volume of 200 μL growth medium in 96-well plates. The undifferentiated cells (UC) and the differentiated cells (DC) were incubated with CPS, CPS-extract, and CPS-extract SLNs at two different concentrations (1 and 0.1 μM). After 24 and 48 h of incubation, the cells both UC and DC were assessed for viability by using a colorimetric assay of 3-[4,5-dimethylthiazol-2-yl]-2,5-diphenyltetrazolium bromide (MTT) test as described by Cacciatore et al. [31]. For experiments with the neurotoxin H_2O_2, the differentiated SH-SY5Y cells were pretreated with CPS, CPS-extract, and CPS-extract SLNs at 0.1 μM for 24 h and then exposed to 25, 150, and 300 μM H_2O_2 for further 24 h. Cell viability was revealed using the MTT assay.

2.11.3. Intracellular reactive oxygen species (ROS) measurement

Intracellular ROS were quantified by the 2′,7′-

dichlorodihydrofluorescein diacetate (H_2DCFDA Cat. No. D6883; Sigma) as described by Sozio et al., 2013 [32], using a Synergy H1, BioTek a microplate reader fluorometer. Briefly, the differentiated SH-SY5Y cells were treated with CPS, CPS-extract, and CPS-extract SLNs at 0.1 μM for 24 h. After the incubation with 10 μM of permeable fluorescent and chemiluminescent probes, the cells were treated with 25 μM H_2O_2 for immediate fluorescence measurement.

2.11.4. Nitro blue tetrazolium chloride (NBT) assay

The differentiated SH-SY5Y cells were treated with CPS, CPS-extract, and CPS-extract SLNs at 0.1 μM for 24 h and then 10^6 cells were detached, centrifuged for 5 min at 1200 rpm, and resuspended in 1 mL of 0.9 % NaCl with 1 mg/mL of NBT (Sigma-Aldrich, Milan, Italy). The spectrophotometric NBT (Nitro blue tetrazolium chloride, assay, conventionally used to determine the production of $O_2^{\bullet-}$ and based on the reduction of NBT in Nitro blue-formazan in the presence of O_2, was performed according to Di Stefano et al. [33].

2.11.5. Statistical analysis

The results of the biological analysis are presented as the mean ± SEM of three different experiments (each $n = 8$). The statistical analysis (unpaired *t*-tests) was carried out using GraphPad Prism Software, version 9.3.1 (GraphPad Software, La Jolla, California, USA), comparing treated cells with respect to the control.

3. Results and discussion

3.1. CPS extraction and quantification

CPS identification was performed by HPLC using the optimized chromatographic conditions by comparing the retention times and chromatograms of CPS in the extract samples with those of reference standards. Fig. 2 shows a chromatogram of the CPS-extract where the highest peak represents the CPS detected at a wavelength of 280 nm. CPS resulted well separated from dihydrocapsaicin (DHC) and nordihydrocapsaicin (*n*-DHC) with retention times of 9.39, 13.68, and 8.63 min, respectively.

The calibration curve of CPS showed a linear relationship within the range of the considered concentrations (2.5–50 μg/mL) with a high correlation coefficient ($R^2 = 0.9991$). The LOD and LOQ, calculated considering the regression equation ($y = 13.601x - 9.5392$), were 3.07 and 9.29 μg/mL, respectively. CSP, as the most abundant extract constituent, was found in a percentage of 52 % over those of *n*-DHC (9 %) and DHC (39 %).

Table 1
Physico-chemical features of CPS-extract SLNs.

	Size (nm)	PDI	ζ-potential (mV)	EE %	Recovery %
Empty SLNs	178.11 (±1.94)	0.02 (±1.91)	−28.7 (±0.76)	–	–
CPS-extract SLNs	208.2 (±10.74)	0.17 (±3.63)	−27.9 (±0.47)	86.27 (±5.14)	61

3.2. CPS-extract SLNs preparation and characterization

CPS-extract SLNs were proposed to overcome CPS biopharmaceutical limitations and increase its targeting in the brain. SLNs were successfully formulated using SA as solid lipid, which was emulsified with the aqueous phase containing Brij 78. Brij 78 is a non-ionic surfactant possessing an attractive hydrophyl-lipophyl balance (HLB) value suitable to form oil-in-water (o/w) microemulsions. The lipid/surfactant phase and the lipid/extract ratios were 1:0.3 and 1:1.5, respectively. These ratios guaranteed the best physico-chemical properties and a CPS-extract solubilization up to 800 μg/mL. Indeed, based on preformulation studies by raising both the lipid and extract amounts, large and highly polydisperse particles were obtained, also macroscopically characterized by turbidity and precipitates (data not shown). In previous work, the effect of SA and Brij 78 was evaluated in a systematic study, which highlighted a close correlation between their concentrations and both size and EE% of the resulting SLNs. The particle size was optimized by using a surfactant: lipid ratio of 0.38:1 [18]. The strong dependency of particle size from the surfactant, is due to the lack of self-emulsifying property of stearic acid in aqueous media. This aspect was well-established by several investigations [34].

CPS-extract SLNs appeared as a homogenous suspension, orange-coloured. They showed a hydrodynamic diameter of 208.2 nm, slightly bigger compared to the empty SLNs (178.11 nm). ζ-potential measurements revealed appreciable negative surface charge with values lower than −20 mV for both blank and CPS-extract SLNs (−28.7 and −27.9 mV before and after loading, respectively) (Table 1). This negative charge is conferred by the SA, organized in the lipid core with the lipophilic hydrocarbon chains, which exposes the –COOH group, expected in its dissociation form at physiological pH, into the aqueous phase. These results suggest good electrostatic stabilization since it is well established that ζ-potential values ranging from +30 and −30 mV indicate physically stable dispersions able to avoid particle aggregation through van der Waals interactions [35,36]. The increase in size, after CPS-extract loading, may confirm the high encapsulation (86 %) even if a small amount of CPS-extract is supposed to be adsorbed on the particle

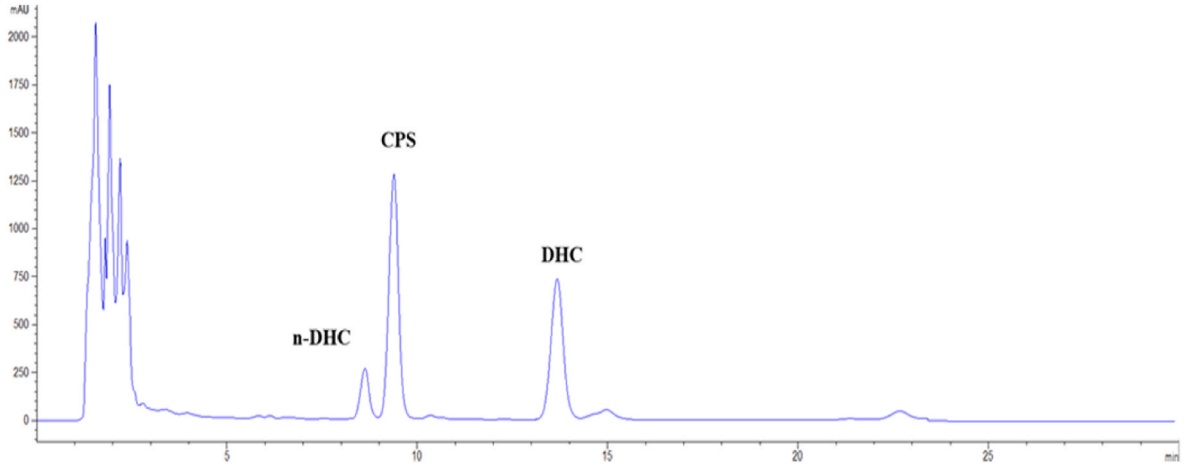

Fig. 2. HPLC chromatogram of CPS-extract.

surface as suggested by the slight decrease of the negative charge in the loaded formulation. Low PDI values of 0.02 and 0.17, before and after loading, suggest uniform and monodisperse formulations characterized by a narrow size distribution [37]. Moreover, CPS-extract SLNs showed an EE% of 86.27, with a recovery, after freeze drying of 61 % (Table 1). The high EE% may be explained by strong hydrophobic interactions established between the fatty acid chains and alkyl chains present in the solid lipid core and the CPS-extract, respectively. Additional intermolecular hydrogen bonds between the Brij 78 hydroxyl groups and the capsaicinoids phenolic and amide groups further immobilize the cargo in the nanostructure. These results suggest physico-chemical properties suitable for the proposed brain delivery. Indeed, particle size, PDI, and ζ-potential are key parameters affecting nanoparticle uptake via transcellular, paracellular transport, and/or nonspecific uptake mechanisms. It has been demonstrated that negatively charged nanoparticles (Nps) may have a unique ability to penetrate the electrostatic BBB. In our case, we also tried to increase the plasma half-life producing particles with a size close to 200 nm corresponding to the best size for an engineered long-circulatory particle which also enables to cross tight endothelial cells of the BBB [22,38,39]. Additionally, we propose a surface coating with the hydrophilic surfactant Brij 78, commonly employed in Nps manufacturing to confer them stealth features. Since its amphiphilic nature, Brij 78 in aqueous media self-assemblies and forms a steric barrier, composed of hydrophilic PEG chains, which shields particles from opsonization, and clearance mechanisms mediated by the reticuloendothelial system (RES) [40]. Beyond this RES escaping, Brij 78 may increase the CPS delivery on the CNS since its ability to open tight junctions without any alteration on the BBB parameters, as confirmed by *in situ* brain perfusion studies [41,42]. These results are supported by several studies described in the literature. In some works, the effect of surfactants has been investigated as a hopeful strategy to prevent aggregation, modify SLN's features, and increase brain drug distribution. In the field of neurodegenerative disorders, andrographolide-loaded SLNs were proposed as potential brain delivery systems [43]. *In vivo* studies performed on healthy rats demonstrated the ability of this kind of formulation to overcome the BBB as confirmed by the fluorescent nanoparticle's detection in the brain parenchyma [39,41]. Brij 78 also promoted in paclitaxel loaded-Nps an improvement of the brain drug distribution related to their ability to circumvent BBB P-gp efflux transporters [44].

3.3. Thermal analysis

DSC is a thermal analysis widely used for the characterization of drug-loaded Nps in terms of crystallinity degree, drug-lipid interactions, and polymorphism. DSC thermograms of the bulk materials and both empty and CPS-extract SLNs are shown in Fig. 3, and the phenomenological data including onset temperature (T_{onset}), melting temperature, and melting enthalpy (ΔH) are reported in Table 2. CPS-extract showed a wide endothermic thermal event from 113 °C, associated with water evaporation. The well-known sharp endothermic melting peak close to 65 °C of the pure CPS, representing its crystalline nature is not detectable in the CPS-extract probably due to its amorphization occurring during the extraction. Both Brij 78 and SA displayed an endothermic transition at 42 °C and 68 °C, respectively. Compared to the bulk materials, CPS-extract SLNs showed a broader peak with a lower onset temperature [45,46]. The wider peak, at lower onset temperature, and the ΔH decline both suggest a less ordered crystal state which may be due to CPS-extract/lipid matrix interactions [47].

Table 2
DSC parameters of CPS-extract SLNs and their constituents.

	T_{onset} (°C)	T_m (°C)	ΔH (J/g)
Stearic Acid	68.375	71.333	206.469
Brij78	42.096	45.666	145.932
CPS-extract	113.004	120.066	38.912
CPS-extract SLNs	58.577	63.000	40.174
Empty SLNs	62.137	66.000	68.857

3.4. Stability studies of CPS-extract SLNs

To define the formulation stabilities their physico-chemical properties were assessed for 30 days at different storage conditions. No significant effects were observed in CPS-extract SLNs stored at 25 and 4 ± 2 °C. As shown in Fig. 4 A, their initial size, after 2 days, slightly increased to around 300 and 250 nm for formulation stored at 25 and 4 °C, respectively.

After these initial changes, these values remained almost stable for a period of at least 30 days, suggesting that SLNs do not lose their integrity but simply undergo a slight structural rearrangement preserving their stability. Concerning the ζ-potentials, the surface charge resulted almost unchanged over 30 days, further supporting the maintained integrity. The residual CPS was also quantified after the incubation period and no significant changes were detected since the drug quantity resulted slightly reduced of around 10 %. These results agree with previous work which proved the good storage shelf-life and storage stability of SLNs loaded herbal extracts [48].

3.5. In vitro drug release

The release rate of CPS from SLNs was studied at room temperature. As shown in Fig. 5, after 24 h it has reached the maximum release of almost 90 %. The release profile is characterized by a gradual release that provides, within 9 h, the release of approximately 80 % of CPS,

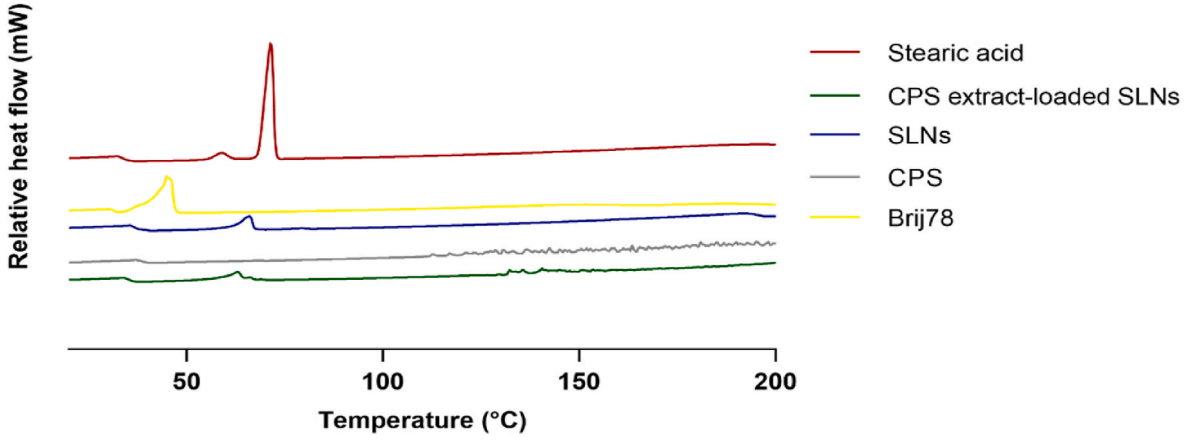

Fig. 3. Thermal analysis of starting materials and CPS-extract SLNs.

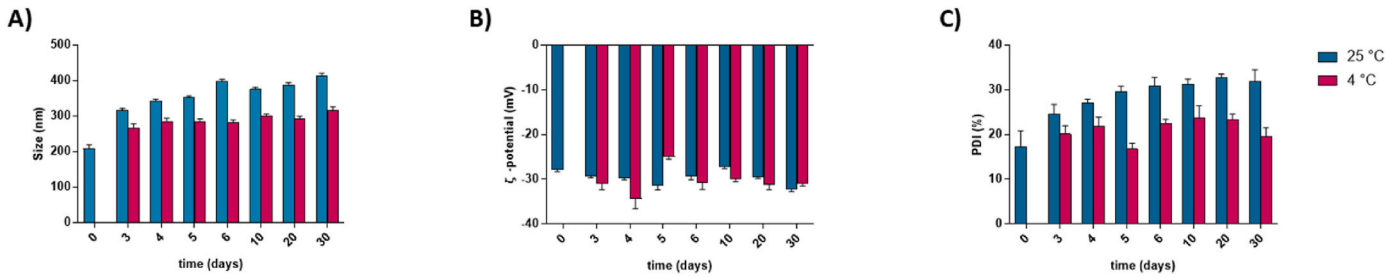

Fig. 4. CPS-extract SLNs stability in the preparation media at different temperatures. Evaluation in terms of particle size (**A**), ζ-potential (**B**), and PDI (**C**) over a period of 30 days. Each value represents the mean ± SD ($n = 3$).

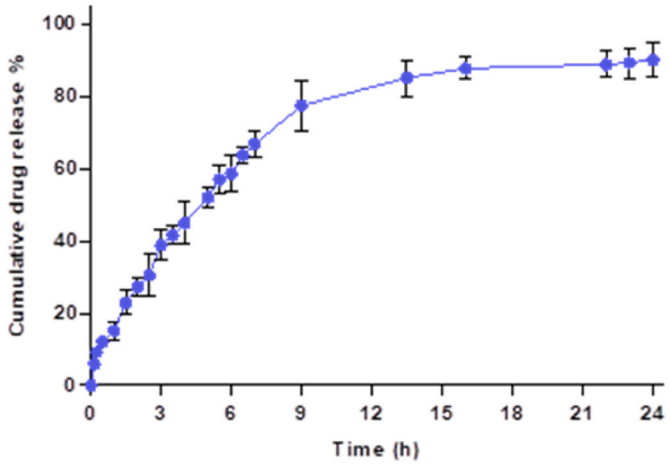

Fig. 5. Release profile of CPS from CPS-extract SLNs.

probably adsorbed on the outer layer of the lipid matrix or interacting with the surfactant shell of the SLNs. After this period, the release rate becomes slower most likely because this phase involves the innermost CPS-extract, included in the core, which needs to cross the lipid matrix through a diffusion process and hindering effect due to the surrounding shell of solid lipid [16]. The release profile may be justified by the high affinity between CPS aromatic moiety and SA involved each other in hydrophobic interactions responsible for the hold back of the CPS-extract thus delaying its release into the aqueous medium. Considering the high affinity with the lipids, CPS-extract may result homogeneously dispersed in the matrix in either an amorphous cluster or molecularly dispersed phase (adsorbed on the SLNs surface and entrapped in the core), a recurring pattern for highly lipophilic drugs incorporated into SLNs [48,49].

The *in vitro* drug release data were fitted into different empirical models including zero-, first-order, Higuchi, and Korsmeyer-Peppas kinetic models [29]. The corresponding kinetic parameters (R^2, k, and n), obtained from the investigated fit models, are reported in Table 3. The highest R^2 value allowed us to define the kinetic which better describes the CPS release from the SLNs. Based on the results the CPS-extract release was best fitted into the Korsmeyer–Peppas model (R^2 = 0.9721). Furthermore, the n value being >0.5 but lower than 1 allows us to define an anomalous, non-Fickian diffusion release, controlled by both diffusion and lipid erosion mechanisms, implied in the control of drug release rate from the lipid core and through the interfacial film formed by the surfactant [50]. These results agree with previously published data involving drug-loaded SLNs where the best fit into the Korsmeyer-Peppas model, with n value ranging from 0.43 to 0.85, were found [51,52]. The CPS release kinetic from CPS-extract SNLs may result in a decrease of its unwanted burning and pungency, in part due to the reduced content (~50 % of CPS) in the entrapped extract, and because of the gradual release that can counteract the undesired effects after a proposed oral administration.

3.6. PAMPA assays

PAMPA assay is based on the evaluation of the passive diffusion through an artificial membrane made of PBL mimicking the physico-chemical microenvironment of the BBB. Results revealed that the permeability of both CPS and CPS-extract are low with *Pe* values of 0.35 ± 0.04 × 10^{-6} and 1.78 ± 0.05 × 10^{-6} cm/s, respectively. For this reason, SLNs were selected as a well-known approach suitable to increase their permeability. Indeed, CPS permeability increased when included in SLNs (Table 4). As expected, dopamine and diazepam selected as standard compounds showed low (Pe < 2 × 10^{-6} cm/s) and high permeability (Pe > 4 × 10^{-6} cm/s), respectively. PAMPA-BBB represents an *in vitro* assay extremely helpful in the early stages of preformulation studies since it considers the worst case underestimating the effective *in vivo* BBB crossing in which more events may allow the active drug uptake [30].

3.7. Biological assays

CPS protects against oxidative insults and alleviates behavioural deficits occurring in PD [10]. Since oxidative stress is one of the key biochemical abnormalities involved in the progression of PD [53], it is

Table 3
Kinetic parameters of the *in vitro* release of CPS-extract from SLNs.

Zero Order $Q_t=Q_0-k_0t$		First Order $\log Q_t=\log Q_0+k_1t/2.303$		Higuchi $Q_t=k_Ht^{1/2}$		Korsmeyer-Peppas $M_t/M_\infty=kt^n$		
R^2	k_0 (h^{-1})	R^2	k_1 (h^{-1})	R^2	k_H($h^{-1/2}$)	R^2	K (h^{-n})	*N*
0.7811	3.4820	0.4373	0.2211	0.9348	20.2390	0.9721	18.9877	0.5630

Qt: amount of active agent released on time *t*; Q_0: initial amount of drug dissolved (equal to zero).
K_0, k_1, k_H, *k*: constants for the zero-, first-order kinetics, Higuchi and Korsmeyer-Peppas models, respectively.
M_∞ amount of drug at the equilibrium state; M_t amount of drug released over time t.
n: exponent release, related to the drug release mechanism.
The constant values of zero order and Higuchi correspond to the slopes of the lines. The constant value for first-order model is obtained from the equation: slope = k/2.303 [28].

Table 4
PAMPA-BBB permeability assays [a].

	PAMPA-BBB permeability *Pe* (10^{-6} cm/s) pH 7.4 [b]	Classification[c]
CPS	0.35 ± 0.04	CNS -
CPS-extract	1.78 ± 0.05	CNS -
CPS-extract SLNs	4.05 ± 0.21	CNS ±

[a] SD range is within ±8 % for all the experiments (each data point represents the mean of three repeats).
[b] pH of both donor and acceptor compartments.
[c] CNS + (high BBB permeation): $Pe > 4.0 \times 10^{-6}$ cm/s; CNS +/− (discrete BBB permeation): *Pe* from 4.0×10^{-6} cm/s to 2.0×10^{-6} cm/s; CNS- (low BBB permeation): $Pe < 2.0 \times 10^{-6}$ cm/s [30].

important to identify specific substances that have an antioxidant and protective effect. Here, we investigated the antioxidant effects of CPS, CPS-extract, CPS-extract SLNs in SH-SY5Y human neuroblastoma cells. To define the appropriate concentration range, the cytotoxic effects of the selected compounds were determined by the MTT test (Fig. 6). Thus, dose–response experiments were performed in both UC (Fig. 6 A) and DC (Fig. 6 B), in concentrations of 1 and 0.1 μM to verify whether, 24 and 48 h after incubation, the compounds had any effect on the cell vitality [54]. The concentration of 0.1 μM was selected to evaluate both the antioxidant and neuroprotective activity since did not interfere with SH-SY5Y cell vitality.

The neuroprotective and antioxidative capacity of CPS, CPS-extract, CPS-extract SLNs against oxidative stress was evaluated by using the human neuroblastoma cell line SH-SY5Y. H_2O_2 was used as a toxic insult on SH-SY5Y cells for the generation of exogenous free radicals to obtain an *in vitro* model of PD. Thus, differentiated SH-SY5Y cells were pre-treated with CPS, CPS-extract, CPS-extract SLNs for 24 h and then

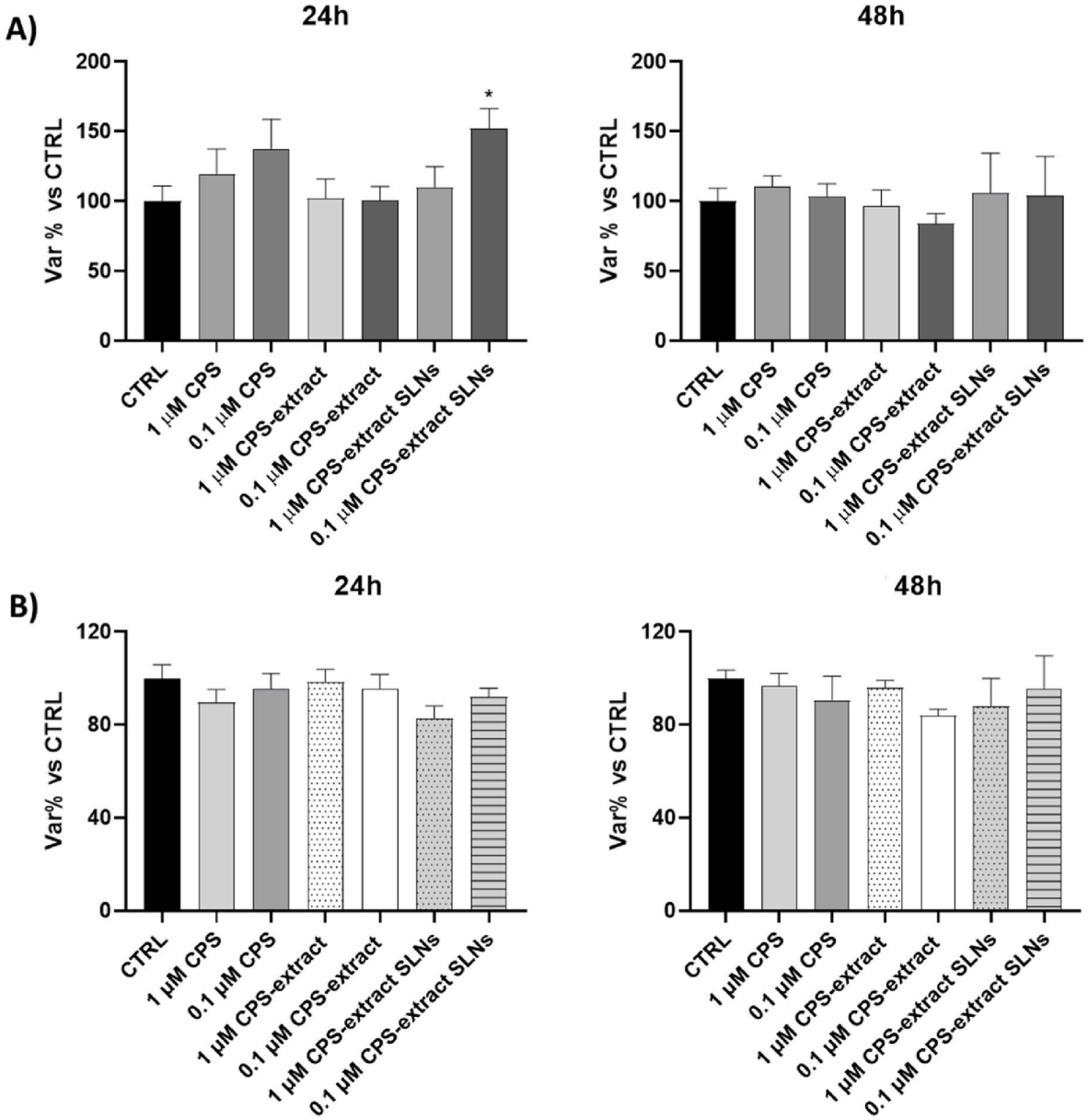

Fig. 6. Dose-response effects of CPS, CPS-extract, CPS-extract SLNs in undifferentiated (**A**) and differentiated (**B**) SH-SY5Y human neuroblastoma cells. The cells were incubated for 24 and 48 h with 1 and 0.1 μM concentrations of the compounds. CTRL: cells w/o compounds. The values are reported as means ± SEM of the percentage variation with respect to CTRL of three different experiments ($n = 16$). *$p < 0.05$.

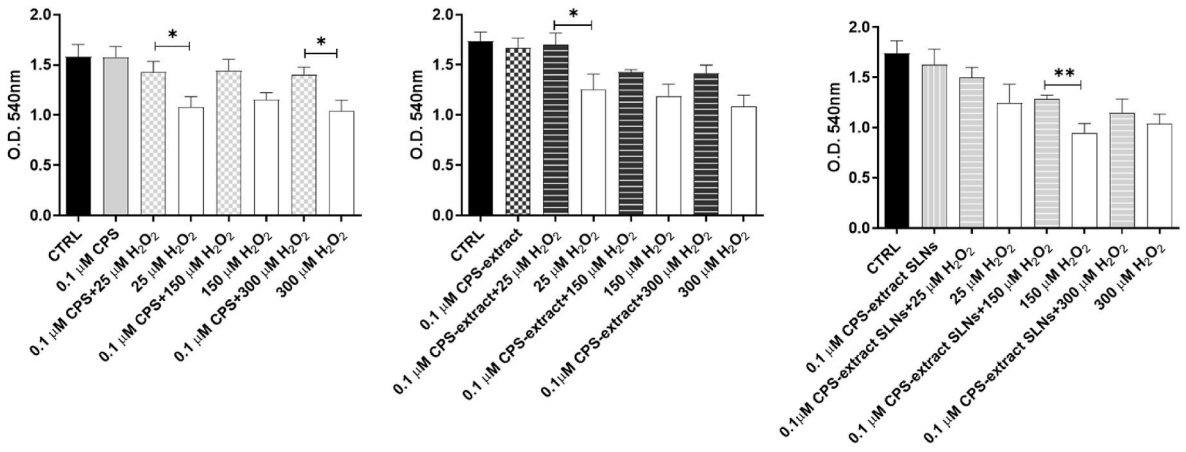

Fig. 7. MTT assay in differentiated and H_2O_2-lesioned SH-SY5Y human neuroblastoma cells in the presence of 0.1 μM CPS, CPS-extract, CPS-extract SLNs. The means ± SEM derived from three different experiments ($n = 16$). *$p < 0.05$; **$p < 0.005$.

exposed to H_2O_2 (25-150-300 μM) for another 24 h. Cell viability was detected using MTT assay as shown in Fig. 7. All the tested samples showed a protective effect against H_2O_2. Moreover, our results indicate that CPS can protect almost completely from the toxic effect of H_2O_2 at all concentrations, maintaining the viability like controls or cells treated with the unentrapped CPS-extract. Otherwise, CPS, CPS-extract, CPS-extract SLNs efficiently counteract the effect of 25 μM H_2O_2, although they exert a partial protective effect on cell viability even at higher H_2O_2 concentrations. The neuroprotection results were more pronounced in presence of the extract instead of pure CPS. This effect could be related to the synergic action of other polyphenols contained in the extract, that, in combination, more efficiently subverts the damage induced by the H_2O_2.

To measure ROS and the cell capability to counteract this insult, H_2DCFDA was used as a specific probe for direct measuring the redox state of a cell. Based on previous results, the concentration of 25 μM H_2O_2 was selected to evaluate the ability of CPS, CPS-extract, CPS-extract SLNs to reduce oxidant levels. Our data showed that all the compounds in the presence of H_2O_2 exerted an antioxidant action, keeping free radical levels lower than the control treated with H_2O_2 and like the control. Moreover, treated SH-SY5Y displayed ROS levels lower than the control (Fig. 8), confirming antioxidant and neuroprotective capabilities.

Furthermore, the antioxidant effects of CPS, CPS-extract, CPS-extract SLNs were assessed also by NBT assay (Fig. 9). The formazan concentration deriving from NBT reduction is determined using a spectrophotometer, such that more formazan indicates that more O_2^- had reduced NBT. In the presence of potent antioxidant substances, the superoxide is detoxified by the scavenger action, which decreases the amount of NBT reduced, allowing the detection of a reduced amount of formazan. Our results showed a significant decrease of O_2^- levels after 24 h of incubation in the presence of CPS, CPS-extract, CPS-extract SLNs at 0.1 μM.

Taking together these results CPS-extract SLNs possessed favorable

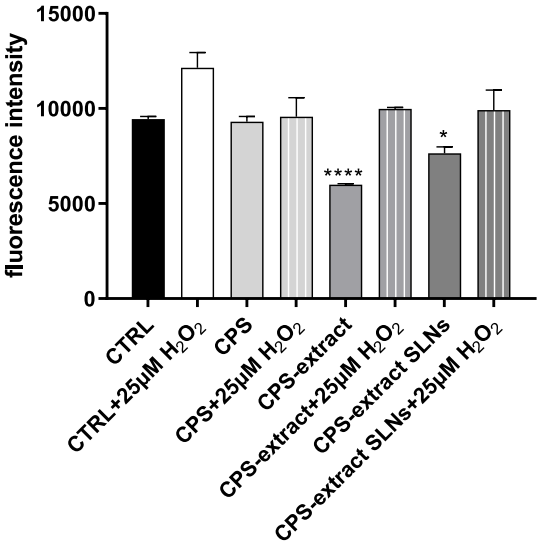

Fig. 8. ROS measurement by H_2DCFDA fluorescence in differentiated SH-SY5Y human neuroblastoma cells exposed to 0.1 μM CPS, CPS-extract, CPS-extract SLNs 24 h before with 25 μM H_2O_2. CTRL: cells w/o compounds. The values are reported as means ± SEM of the fluorescence intensity, derived from three different experiments ($n = 8$). *$p < 0.05$; ****$p < 0.0001$.

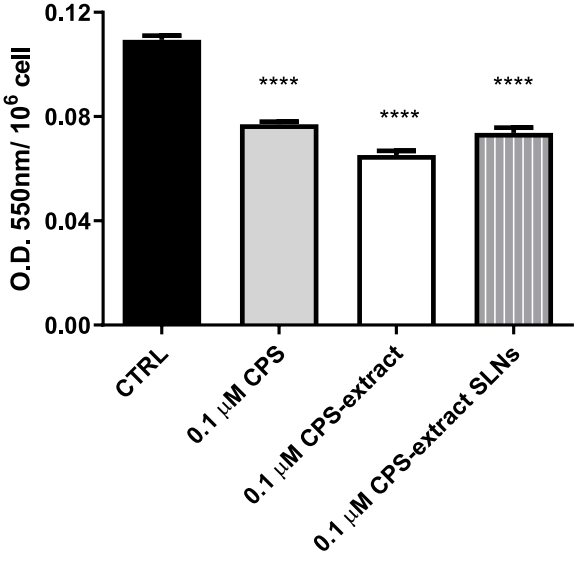

Fig. 9. NBT assay in differentiated SH-SY5Y human neuroblastoma cells, in the presence of 0.1 μM CPS, CPS-extract, CPS-extract SLNs, after 24 h of incubation. Mean values ± SEM were derived from three independent experiments ($n = 5$; ****$p < 0.0001$, Unpaired *t*-test). CTRL: cells w/o compounds *vs* treated cells for 24 h.

features and a significant protective effect in reducing ROS increments. This evidence suggests that the proposed formulation may be considered a suitable nanomedical tool to manage PD also through the modulation of gut inflammation, closely associated with the pathogenesis of this neurodegenerative disease [55].

4. Conclusion

In this study, the feasibility of SLNs for CPS extract delivery was assessed. The optimized CPS-extract SLNs, prepared using SA and Brij 78, showed advantageous physicochemical properties, suitable for the intended purpose, and provided a gradual release of CPS, increasing its bioavailability in the brain. Moreover, biological studies revealed that CPS as well as the derived formulation tested, at sufficiently low and physiological concentrations used, provides a significant antioxidant capacity by protecting dopaminergic-like cells from oxidant insults. This preliminary data indicates that CPS-extract SLNs represent a promising strategy to overcome the BBB as suggested by the PAMPA-BBB assays. These results warrant further efforts to clarify the uptake mechanisms in greater detail. Proof of the concept will involve an investigation of CPS-extract SLNs *in vivo* neuroprotective profile.

Funding

This research was funded by the finanziato dall'Unione europea – NextGenerationEU, MUR-Fondo Promozione e Sviluppo - DM 737/2021, TAAGID, Novel Terpenoid-prodrugs with antimicrobial and anti-inflammatory activities for the treatment of severe gastrointestinal diseases.

Author statement

Lisa Marinelli: Conceptualization, Supervision, Methodology, Writing- Reviewing and Editing;

Marilisa Pia Dimmito: Data curation, Supervision, Writing- Original draft preparation, Funding acquisition;

Ivana Cacciatore: Supervision, Visualization, Writing- Reviewing and Editing;

Eleonora Chiara Toto: Investigation, Conceptualization, Methodology;

Annalisa Di Rienzo: Investigation, Data curation, Methodology;

Ferdinando Palmerio: Investigation, Data curation, Methodology;

Valentina Puca: Investigation, Data curation, Methodology;

Ester Sara Di Filippo: Data curation, Methodology, Investigation;

Stefania Fulle: Supervision, Visualization, Writing- Reviewing and Editing;

Antonio Di Stefano: Project administration, Supervision, Visualization, Writing- Reviewing and Editing.

Declaration of competing interest

The authors declare that they have no known competing financial interests or personal relationships that could have appeared to influence the work reported in this paper.

Data availability

No data was used for the research described in the article.

Appendix A. Supplementary data

Supplementary data to this article can be found online at https://doi.org/10.1016/j.jddst.2023.105097.

References

[1] Z. Mari, T.A. Mestre, The disease modification conundrum in Parkinson's disease: failures and hopes, Front. Aging Neurosci. 14 (2022) 1–7, https://doi.org/10.3389/fnagi.2022.810860.

[2] A. Di Stefano, B. Mosciatti, G.M. Cingolani, G. Giorgioni, M. Ricciutelli, I. Cacciatore, P. Sozio, F. Claudi, Dimeric L-dopa derivatives as potential prodrugs, Bioorg. Med. Chem. Lett 11 (2001) 1085–1088, https://doi.org/10.1016/s0960-894x(01)00140-8.

[3] T.K. Lee, E.L. Yankee, A review on Parkinson's disease treatment, Neuroimmunol. Neuroinflammation 8 (2022) 222, https://doi.org/10.20517/2347-8659.2020.58.

[4] B.D. Li, Z.Y. Bi, J.F. Liu, W.J. Si, Q.Q. Shi, L.P. Xue, J. Bai, Adverse effects produced by different drugs used in the treatment of Parkinson's disease: a mixed treatment comparison, CNS Neurosci. Ther. 23 (2017) 827–842, https://doi.org/10.1111/cns.12727.

[5] F. Pohl, P.K.T. Lin, The potential use of plant natural products and plant extracts with antioxidant properties for the prevention/treatment of neurodegenerative diseases: in vitro, in vivo and clinical trials, Molecules 23 (2018) 3283, https://doi.org/10.3390/molecules23123283.

[6] M. Ilie, C. Caruntu, M. Tampa, S.-R. Georgescu, C. Matei, C. Negrei, R.-M. Ion, C. Constantin, M. Neagu, D. Boda, Capsaicin: physicochemical properties, cutaneous reactions and potential applications in painful and inflammatory conditions (Review),, Exp. Ther. Med. (2019) 916–925, https://doi.org/10.3892/etm.2019.7513.

[7] S. Basith, M. Cui, S. Hong, S. Choi, Harnessing the therapeutic potential of capsaicin and its analogues in pain and other diseases, Molecules 21 (2016) 966, https://doi.org/10.3390/molecules21080966.

[8] A. Akhtar, A. Andleeb, T.S. Waris, M. Bazzar, A.R. Moradi, N.R. Awan, M. Yar, Neurodegenerative diseases and effective drug delivery: a review of challenges and novel therapeutics, J. Contr. Release 330 (2021) 1152–1167, https://doi.org/10.1016/j.jconrel.2020.11.021.

[9] Y.C. Chung, J.Y. Baek, S.R. Kim, H.W. Ko, E. Bok, W.H. Shin, S.Y. Won, B.K. Jin, Capsaicin prevents degeneration of dopamine neurons by inhibiting glial activation and oxidative stress in the MPTP model of Parkinson's disease, Exp. Mol. Med. 49 (2017) e298–e299, https://doi.org/10.1038/emm.2016.159.

[10] J. Liu, H. Liu, Z. Zhao, J. Wang, D. Guo, Y. Liu, Regulation of Actg1 and Gsta2 is possible mechanism by which capsaicin alleviates apoptosis in cell model of 6-OHDA-induced Parkinson's disease, Biosci. Rep. 40 (2020) 1–12, https://doi.org/10.1042/BSR20191796.

[11] E. Bok, Y.C. Chung, K.S. Kim, H.H. Baik, W.H. Shin, B.K. Jin, Modulation of M1/M2 polarization by capsaicin contributes to the survival of dopaminergic neurons in the lipopolysaccharide-lesioned substantia nigra in vivo, Exp. Mol. Med. 50 (2018) 1–14, https://doi.org/10.1038/s12276-018-0111-4.

[12] O.M.E. Abdel-Salam, A.A. Sleem, M.A.E.B.M. Sayed, E.R. Youness, N. Shaffie, Capsaicin exerts anti-convulsant and neuroprotective effects in pentylenetetrazole-induced seizures, Neurochem. Res. 45 (2020) 1045–1061, https://doi.org/10.1007/s11064-020-02979-3.

[13] Y.H. Siddique, F. Naz, S. Jyoti, Effect of capsaicin on the oxidative stress and dopamine content in the transgenic drosophila model of Parkinson's disease, Acta Biol. Hung. 69 (2018) 115–124, https://doi.org/10.1556/018.69.2018.2.1.

[14] W.D. Rollyson, C.A. Stover, K.C. Brown, H.E. Perry, C.D. Stevenson, C.A. McNees, J.G. Ball, M.A. Valentovic, P. Dasgupta, Bioavailability of capsaicin and its implications for drug delivery, J. Contr. Release 196 (2014) 96–105, https://doi.org/10.1016/j.jconrel.2014.09.027.

[15] A.R. Ahmady, A. Solouk, S. Saber-Samandari, S. Akbari, H. Ghanbari, B.E. Brycki, Capsaicin-loaded alginate nanoparticles embedded polycaprolactone-chitosan nanofibers as a controlled drug delivery nanoplatform for anticancer activity, J. Colloid Interface Sci. 638 (2023) 616–628.

[16] L.Y. Zhuang, H. Zhang, N. Tian, W. Dang, S. Wu, Capsaicin-loaded folic acid-conjugated lipid nanoparticles for enhanced therapeutic efficacy in ovarian cancers, Biomed. Pharmacother. 91 (2017) 999–1005.

[17] S. Kunjiappan, M. Sankaranarayanan, B.K. Kumar, P. Pavadai, E. Babkiewicz, P. Maszczyk, E. Glodkowska-Mrowka, S. Arunachalam, S.R.K. Pandian, V. Ravishankar, S. Baskararaj, S. Vellaichamy, L. Arulmani, T. Panneerselvam, Capsaicin-loaded solid lipid nanoparticles: design, biodistribution, in silico modeling and in vitro cytotoxicity evaluation, Nanotechnology 32 (2021), 095101.

[18] S. Laserra, A. Basit, P. Sozio, L. Marinelli, E. Fornasari, I. Cacciatore, M. Ciulla, H. Türkez, F. Geyikoglu, A. Di Stefano, Solid lipid nanoparticles loaded with lipoyl–memantine codrug: preparation and characterization, Int. J. Pharm. 485 (2015) 183–191, https://doi.org/10.1016/j.ijpharm.2015.03.001.

[19] R. Ben Khalifa, I. Cacciatore, M.P. Dimmito, M. Ciulla, R. Grande, V. Puca, I. Robuffo, V. De Laurenzi, L. Chekir-Ghedira, A. Di Stefano, L. Marinelli, Multiple lipid nanoparticles as antimicrobial drug delivery systems, J. Drug Deliv. Sci. Technol. 67 (2022), 102887, https://doi.org/10.1016/j.jddst.2021.102887.

[20] N.H. Khan, M. Mir, E.E. Ngowi, U. Zafar, M.M.A.K. Khakwani, S. Khattak, Y. K. Zhai, E.S. Jiang, M. Zheng, S.F. Duan, J.S. Wei, D.D. Wu, X.Y. Ji, Nanomedicine: a promising way to manage alzheimer's disease, Front. Bioeng. Biotechnol. 9 (2021), 630055, https://doi.org/10.3389/fbioe.2021.630055.

[21] Y. Duan, A. Dhar, C. Patel, M. Khimani, S. Neogi, P. Sharma, N. Siva Kumar, R. L. Vekariya, A brief review on solid lipid nanoparticles: Part and parcel of contemporary drug delivery systems, RSC Adv. 10 (2020) 26777–26791, https://doi.org/10.1039/d0ra03491f.
[22] M.K. Satapathy, T. Yen, J. Jan, R. Tang, J. Wang, R. Taliyan, C. Yang, Solid lipid nanoparticles (SLNs): an advanced drug delivery system targeting brain through BBB, Pharmaceutics (2021) 1–36.
[23] Y.Y.C. Tam, S. Chen, P.R. Cullis, Advances in lipid nanoparticles for siRNA delivery, Pharmaceutics 5 (2013) 498–507, https://doi.org/10.3390/pharmaceutics5030498.
[24] D.W.G. Harron, Technical requirements for registration of pharmaceuticals for human use: the ICH process, Textbook Pharmaceut. Med. 1994 (2013) 447–460, https://doi.org/10.1002/9781118532331.ch23.
[25] Y. Shi, M.J. van Steenbergen, E.A. Teunissen, L. Novo, S. Gradmann, M. Baldus, C. F. van Nostrum, W.E. Hennink, Π-π stacking increases the stability and loading capacity of thermosensitive polymeric micelles for chemotherapeutic drugs, Biomacromolecules 14 (2013) 1826–1837, https://doi.org/10.1021/bm400234c.
[26] G. Quiram, F. Montagner, K.L. Palmer, M.C. Stefan, K.E. Washington, D. C. Rodrigues, Novel chlorhexidine-loaded polymeric nanoparticles for root canal treatment, J. Funct. Biomater. 9 (2018) 29, https://doi.org/10.3390/jfb9020029.
[27] A.R. Chandrasekaran, C.Y. Jia, C.S. Theng, T. Muniandy, S. Muralidharan, S. A. Dhanaraj, In vitro studies and evaluation of metformin marketed tablets-Malaysia, J. Appl. Pharmaceut. Sci. 1 (2011) 214–217.
[28] Mathematical Models of Drug Release, Strategies to Modify the Drug Release from Pharmaceutical Systems. (2015) vols. 63-86, https://doi.org/10.1016/b978-0-08-100092-2.00005-9.
[29] P.K. Mante, N.O. Adomako, P. Antwi, N.K. Kusi-Boadum, N. Osafo, Solid-lipid nanoparticle formulation improves antiseizure action of cryptolepine, Biomed. Pharmacother. 137 (2021), 111354, https://doi.org/10.1016/j.biopha.2021.111354.
[30] L. Di, E.H. Kerns, K. Fan, O.J. McConnell, G.T. Carter, High throughput artificial membrane permeability assay for blood-brain barrier, Eur. J. Med. Chem. 38 (2003) 223–232, https://doi.org/10.1016/S0223-5234(03)00012-6.
[31] I. Cacciatore, E. Fornasari, L. Baldassarre, C. Cornacchia, S. Fulle, E.S. Di Filippo, T. Pietrangelo, F. Pinnen, A potent (R)-alpha-bis-lipoyl derivative containing 8-hydroxyquinoline scaffold: synthesis and biological evaluation of its neuroprotective capabilities in SH-SY5Y human neuroblastoma cells, Pharmaceuticals 6 (2013) 54–69, https://doi.org/10.3390/ph6010054.
[32] P. Sozio, L.S. Cerasa, S. Laserra, I. Cacciatore, C. Cornacchia, E.S. Di Filippo, S. Fulle, A. Fontana, A. Di Crescenzo, M. Grilli, M. Marchi, A. Di Stefano, Memantine-sulfur containing antioxidant conjugates as potential prodrugs to improve the treatment of Alzheimer's disease, Eur. J. Pharmaceut. Sci. 49 (2013) 187–198, https://doi.org/10.1016/j.ejps.2013.02.013.
[33] A. Di Stefano, L. Marinelli, P. Eusepi, M. Ciulla, S. Fulle, E.S. Di Filippo, L. Magliulo, G. Di Biase, I. Cacciatore, Synthesis and biological evaluation of novel selenyl and sulfur-L-Dopa derivatives as potential anti-Parkinson's disease agents, Biomolecules 9 (2019) 1–13, https://doi.org/10.3390/biom9060239.
[34] S. Kumar, J.K. Randhawa, Solid lipid nanoparticles of stearic acid for the drug delivery of paliperidone, RSC Adv. 5 (2015) 68743–68750, https://doi.org/10.1039/c5ra10642g.
[35] R.M. Shah, F. Malherbe, D. Eldridge, E.A. Palombo, I.H. Harding, Physicochemical characterization of solid lipid nanoparticles (SLNs) prepared by a novel microemulsion technique, J. Colloid Interface Sci. 428 (2014) 286–294, https://doi.org/10.1016/j.jcis.2014.04.057.
[36] M.R. Aji Alex, A.J. Chacko, S. Jose, E.B. Souto, Lopinavir loaded solid lipid nanoparticles (SLN) for intestinal lymphatic targeting, Eur. J. Pharmaceut. Sci. 42 (2011) 11–18, https://doi.org/10.1016/j.ejps.2010.10.002.
[37] P. Adhikari, P. Pal, A.K. Das, S. Ray, A. Bhattacharjee, B. Mazumder, Nano lipid-drug conjugate: an integrated review, Int. J. Pharm. 529 (2017) 629–641, https://doi.org/10.1016/j.ijpharm.2017.07.039.
[38] H. Yuan, J. Miao, Y.Z. Du, J. You, F.Q. Hu, S. Zeng, Cellular uptake of solid lipid nanoparticles and cytotoxicity of encapsulated paclitaxel in A549 cancer cells, Int. J. Pharm. 348 (2008) 137–145, https://doi.org/10.1016/j.ijpharm.2007.07.012.
[39] J.A. Loureiro, S. Andrade, A. Duarte, A.R. Neves, J.F. Queiroz, C. Nunes, E. Sevin, L. Fenart, F. Gosselet, M.A.N. Coelho, M.C. Pereira, N. Latruffe, Resveratrol and grape extract-loaded solid lipid nanoparticles for the treatment of Alzheimer's disease, Molecules 22 (2017) 1–16, https://doi.org/10.3390/molecules22020277.
[40] A.C. Correia, A.R. Monteiro, R. Silva, J.N. Moreira, J.M. Sousa Lobo, A.C. Silva, Lipid nanoparticles strategies to modify pharmacokinetics of central nervous system targeting drugs: crossing or circumventing the blood–brain barrier (BBB) to manage neurological disorders, Adv. Drug Deliv. Rev. 189 (2022), 114485, https://doi.org/10.1016/j.addr.2022.114485.
[41] G. Tosi, T. Musumeci, B. Ruozi, C. Carbone, D. Belletti, R. Pignatello, M. Angela, G. Puglisi, Journal of Drug Delivery Science and Technology the "fate" of polymeric and lipid nanoparticles for brain delivery and targeting: strategies and mechanism of blood e brain barrier crossing and trafficking into the central nervous system, J. Drug Deliv. Sci. Technol. 32 (2016) 66–76, https://doi.org/10.1016/j.jddst.2015.07.007.
[42] S.-H. Hsu, S.A. Al-Suwayeh, C.-C. Chen, C.-H. Chi, J.-Y. Fang, PEGylated liposomes incorporated with nonionic surfactants as an apomorphine delivery system targeting the brain: in vitro release and in vivo real-time imaging, Curr. Nanosci. 7 (2011) 191–199, https://doi.org/10.2174/157341311794653686.
[43] S. Shrivastava, C.D. Kaur, Development of andrographolide-loaded solid lipid nanoparticles for lymphatic targeting: formulation, optimization, characterization, in vitro, and in vivo evaluation, Drug Deliv. Transl. Res. 13 (2023) 658–674, https://doi.org/10.1007/s13346-022-01230-6.
[44] J.M. Koziara, P.R. Lockman, D.D. Allen, R.J. Mumper, Paclitaxel nanoparticles for the potential treatment of brain tumors, J. Contr. Release 99 (2004) 259–269, https://doi.org/10.1016/j.jconrel.2004.07.006.
[45] V. Teeranachaideekul, T. Chantaburanan, V.B. Junyaprasert, Influence of state and crystallinity of lipid matrix on physicochemical properties and permeation of capsaicin-loaded lipid nanoparticles for topical delivery, J. Drug Deliv. Sci. Technol. 39 (2017) 300–307, https://doi.org/10.1016/j.jddst.2017.04.003.
[46] P. Anantaworasakul, W. Chaiyana, B.B. Michniak-Kohn, W. Rungseevijitprapa, C. Ampasavate, Enhanced transdermal delivery of concentrated capsaicin from chili extract-loaded lipid nanoparticles with reduced skin irritation, Pharmaceutics 12 (2020) 463, https://doi.org/10.3390/pharmaceutics12050463.
[47] D.Z. Hou, C.S. Xie, K.J. Huang, C.H. Zhu, The production and characteristics of solid lipid nanoparticles (SLNs), Biomaterials 24 (2003) 1781–1785, https://doi.org/10.1016/S0142-9612(02)00578-1.
[48] D.A. Campos, A.R. Madureira, B. Sarmento, M.M. Pintado, A.M. Gomes, Technological stability of solid lipid nanoparticles loaded with phenolic compounds: drying process and stability along storage, J. Food Eng. 196 (2017) 1–10, https://doi.org/10.1016/j.jfoodeng.2016.10.009.
[49] V. Mishra, K.K. Bansal, A. Verma, N. Yadav, S. Thakur, K. Sudhakar, J. M. Rosenholm, Solid lipid nanoparticles: emerging colloidal nano drug delivery systems, Pharmaceutics 18 (2018) 191, https://doi.org/10.3390/pharmaceutics10040191.
[50] K.W. Wu, C. Sweeney, N. Dudhipala, P. Lakhani, N.D. Chaurasiya, B.L. Tekwani, S. Majumdar, Primaquine loaded solid lipid nanoparticles (SLN), nanostructured lipid carriers (NLC), and nanoemulsion (NE): effect of lipid matrix and surfactant on drug entrapment, in vitro release, and ex vivo hemolysis, AAPS PharmSciTech 22 (2021) 240, https://doi.org/10.1208/s12249-021-02108-5.
[51] J. Xu, B. Xu, D. Shou, X. Xia, Y. Hu, Preparation and evaluation of vancomycin-loaded N-trimethyl chitosan nanoparticles, Polymers 7 (2015) 1850–1870, https://doi.org/10.3390/polym7091488.
[52] H. Amekyeh, N. Billa, Lyophilized drug-loaded solid lipid nanoparticles formulated with beeswax and theobroma oil, Molecules 26 (2021) 1–13, https://doi.org/10.3390/molecules26040908.
[53] Z.X. Zhao, J.F. Wang, L.L. Wang, X.M. Yao, Y.L. Liu, Y. Li, S. Chen, T. Yue, X. T. Wang, W.F. Yu, Y.M. Liu, Capsaicin protects against oxidative insults and alleviates behavioral deficits in rats with 6-OHDA-induced Parkinson's disease via activation of TRPV1, Neurochem. Res. 42 (2017) 3431–3438, https://doi.org/10.1007/s11064-017-2388-4.
[54] J.C. Stockert, A. Blázquez-Castro, M. Cañete, R.W. Horobin, Á. Villanueva, MTT assay for cell viability: intracellular localization of the formazan product is in lipid droplets, Acta Histochem. 114 (2012) 785–796, https://doi.org/10.1016/j.acthis.2012.01.006.
[55] Q.Q. Chen, C. Haikal, W. Li, J.Y. Li, Gut inflammation in association with pathogenesis of Parkinson's disease, Front. Mol. Neurosci. 12 (2019) 218, https://doi.org/10.3389/fnmol.2019.00218.